The Association of Professional Women Engineers of Nigeria

APWEN

JOURNAL OF ENGINEERING, SCIENCE AND TECHNOLOGY

Volume 6, Issue 1 – December 2022

ISSN: 2714-2396

https://www.apwen.org/apwen-journal

APWEN Journal of Engineering, Science, and Technology

Volume 6, Issue 1. 2022

Publication of the Association of Professional Women Engineers of Nigeria

APWEN JOURNAL EDITORIAL ADVISORY BOARD

It is a condition of publication in this APWEN journal that manuscripts have not been published or submitted for publication and will not be submitted or published elsewhere.

Upon the acceptance of articles to be published in this journal, the author(s) are required to transfer the copyright of the article to the publisher.

ISSN: 2714-2396

Published by APWEN Journals,
SUITE 5, GROUND FLOOR, NATIONAL ENGINEERING CENTER,
1, ENGINEERING CLOSE, OFF IDOWU TAYLOR STREET,
VICTORIA ISLAND LAGOS

Printed by APWEN Press

Table of Content of Published Articles

Journal of Engineering, Science, and Technology
ISSN: 2714-2396 | Volume 6, Issue 1

Green synthesis of zinc oxide nanoparticles (ZnONPs) from cassava leaf (Manihot *esculenta*) and its application as a corrosion inhibitor for mild steel in 1M hydrochloric acid

A.O. Okewale[1] and B.H Akpeji[2]

Department of Chemical Engineering, Federal University of Petroleum Resources, PMB 1221, Effurun, Delta State, Nigeria.[2]Department of Chemistry, Federal University of Petroleum Resources, PMB 1221, Effurun, Delta State, Nigeria.
Corresponding author: A.O.Okewale, Department of Chemical Engineering, Federal University of Petroleum Resources,Okewale.akindele@fupre.edu.ng Tel: +2348069365637

Abstract
Corrosion inhibition behaviour of metallic and semiconductor of Zinc Oxide Nanoparticles ZnONPs synthesized through biological means has been extensively reported. This work focuses on the synthesis of zinc oxide nanoparticles from cassava leaf (CL-ZnONPs) and has investigated its efficiency as corrosion inhibitor on mild steel in 1M HCl. The optical and structural properties of the resulting zinc oxide nanoparticles were studied using; UV-visible spectroscopy, Tauc's plot and Fourier transform Infrared spectroscopy (FTIR). The UV–Vis spectra of the zinc oxide nanoparticles showed typical absorption peaks around 371nm due to its large excitation binding energy at room temperature. The FTIR spectra affirmed the presence of –OH, C=C, N=C=S, and C=O functional groups.Gravimetric method was used to study the mild steel corrosion process with a view to evaluating inhibition efficiency of the zinc oxide nanoparticles in 1M HCl. The effects of inhibitor concentration and immersion time were studied at 303 K. The results showed that the efficiency of inhibition increased with immersion time but decreased with inhibitor concentration. The maximum inhibition efficiency was obtained at 120hours (t_{max}) with inhibitor concentration of 100ppm. It was revealed that the mild steel surface is susceptible to acidic corrosion, thus, an increase inconcentration of inhibitor and immersion time significantly influenced the pattern of corrosion.
Keywords: Nanoparticles, CL-ZnO NPs, Cassava Leaf (*Manihot esculenta*), Bio-synthesis, Inhibition efficiency.

Introduction
Recent advancements have been utterly significant in refining, development and implementation of techniques and strategies in metal corrosion management. Nanotechnology has as well ushered in a supporting, innovative and technological standpoint in this regard. In general, nanotechnology involves the atomic manipulation of matter to synthesize new structures, materials, systems, catalysts and devices that show new phenomena and characteristics. Nanotechnology offers the possibility of enhancing the inherent corrosion resistance, extending service life, reducing downtimes and overall performance of process equipment in ways that are cost effective and environmentally benign.
Nanoparticles have been the main focus of the majority of research into nanotechnology, which is largely due to the ease at which they can be prepared and manipulated [1], described the nanoparticle as being capable of bridging the gap between bulk materials and atomic or molecular structures. [2], defined the nanoscale as a theurgic point on the dimensional scale, where the properties of a material in the nanoscale would grossly deviate from that of those

materials at larger scales. [3], proposed the "quantum size effect" as a phenomenon created by the enhanced ratio of surface area to volume of particles as they exist in nanoscale. [4], noted that the enhanced ratio of surface area to volume, interfacial and surface chemistry were capable of giving materials in nanoscale more advantage in chemical reactions such as in catalysis.
According to [5], the physical and chemical methods of nanoparticle synthesis were very much conventional; yet, both methods came with a number of limitations such as the use of toxic compounds, highly endothermic reactions with a high demand for pressure and time as well. [6], in a study explained that the ability to transform inorganic metal ions to metal nanoparticles in biological organisms including humans was possible via the reductive capabilities of the proteins and metabolites present in the organisms. Although, they argued that using plants as a source of nanoparticle synthesis was of an advantage over other biological systems, as plants are readily available with a less tedious and cost effective biogenic synthesis procedure.Metal and metal oxide nanoparticles tend to exhibit interesting chemical properties due to their particle size and surface density. Physical, chemical and biological methods in the synthesis of nanostructured oxides all considers ZnO NPS to exhibit wide band gap (~3.4eV) and large exciton binding energy (60meV) which is responsible for wide range of applications especially in; nano-optoelectronics, transistors, nano-piezoelectronics, sensors and UV-detection. It is on this background that the authors were motivated to synthesize the zinc oxide cassava leaf nanoparticles and also tested its corrosion inhibition potential on mild steel surface in acidic medium with a view to establishing the mode of adsorption process, and its thermodynamic parameter at 303 K.

Materials and Methods

Reagents

Cassava Leaves (*Manihot esculenta*), Zinc Acetate dihydrate, Sodium Hydroxide, Hydrochloric acid, Ethanol, Acetone.

Materials

Mild steel, Whatman filter paper,magnetic stirrers, test tubes, petri-dishes, silicon carbide abrasive paper of various grit sizes, analytical weighing balance($\pm 0.0001\ g$ accuracy), beakers with sizes between 100-1000ml holding capacity, desiccators, centrifuge, industrial blender,and drying oven (LD-201-E Vision Scientific).The Coupons were dimension into 40 mm × 20 mm × 2 mm and cleaned with abrasive paper. A hole of 0.1 cm was drilled on each of the coupon before polishing so as to help in its suspension in acid medium.

Method

2.1 Extraction and Phytochemical Screening of Cassava Leaf

The procedure of extraction and phytochemical screening was performed in accordance with the processes laid out by [7; 8]. The screening of the extract was carried out to identify the main groups of active chemical constituents present in the extract by their colour reaction. The presence of saponins, alkaloids, terpenes, flavonoids, glycosides, reducing sugars and tannins were tested for by simple qualitative and quantitative methods.

2.2 Green synthesis of ZnONPs from Cassava Leaf (*Manihot esculenta)*

2.2.1 Preparation of Plant Extract

The Cassava (*M. esculenta*) leaves were collected from farmers within Iterigbi community in Delta State, Nigeria. The leaves were washed several times with double distilled water to remove any debris or particulates carried along during collection of leaves and then air-dried at room temperature for 72 hours. The Cassava leaves were afterwards pulverized with a standard electric blender and sieved using a Laboratory Test sieve with aperture of 600microns. Dried pulverized leaves of 2g was used in preparing the aqueous extract in 500 ml distilled water and heated at 80 °C for about 1hr. The extracting mixture displayed a colour change in its aqueous solution from watery to yellow. The extract was separated by filtration, using the Whatman™ filter paper and stored in Polyethylene Terephthalate (PET) bottles in order to be used for further synthesis of ZnO nanoparticles.

2.2.2 Preparation of 0.01M Zinc Acetate

The analytical grade Zinc Acetate used in this synthesis was procured from Rovet Scientific Laboratories Benin, Nigeria. 0.01M solution of Zinc Acetate ($Zn(CH3COO)_2.2H_2O$) was prepared by the dissolution of 2.195g Zinc Acetate in 1000ml distilled water.

2.2.3 Preparation of 1M NaOH

Similarly, 1M solution of Sodium Hydroxide (NaOH) was prepared by weighing 40g of NaOH pellets and subsequently dissolved in 1000 ml distilled water.

2.2.4 Preparation of 1M HCI

The molar strength of HCl stock was determined using equation 1 below;

$$\text{Molar strength of HCl stock} = \frac{\text{Percentage purity of HCl} \times \text{Specific gravity of HCl} \times 10}{\text{Molecular Weight of HCl}} \quad (1)$$

Where percentage purity of HCl = 37 %, specific gravity of HCl = 1.08 g/cm^3, and molecular weight of HCl = 36.46 g/mol. Inserting these values in equation (1) above the resulting molar strength value of 11.269 M was obtained. Making use of serial dilution formula as indicated in equation (2) below;

$$C_1V_1 = C_2V_2 \quad (2)$$

Where, C_1 = Concentration of stock HCl (11.269 M), V_1 = Volume required from the stock, C_2 = Concentration required for preparation (1 M), and V_2 is the volume required for preparation of 1 M which is 1 L or 1000 mL. Therefore, 88.7 mL of HCl was measured from the stock bottle and was poured into 1000 mL volumetric flask previously containing some quantity of distilled water. After which, the solution was made up to the mark with distilled water.

2.2.5 Synthesis of Zinc Oxide Nps from Cassava Leaf (GLZnONps)

The procedure of extraction and synthesis was in accordance to the methods of [9, 10] with slight modifications.In this synthesis procedure, 50ml of the aqueous extract of Cassava leaves (*M. esculenta*) and 100ml of 0.01M zinc acetate solution were mixed together with 25ml of 1M NaOH solution that was added drop-wise. The resulting mixture was then mixed by continuously stirring on a magnetic stirrer at a temperature of 70°C for 3hours. During this reaction time, the colour of the colloidal solution gradually changed from yellow to a cream-coloured solution which suggest an increased rate of bio-reduction of the Zinc Acetate and the formation of Zinc Hydroxide ($Zn(OH)_2$) precipitate.

2.2.6 Purification of ZnO Nps

The $Zn(OH)_2$ formed as precipitate was purified by washing with distilled water and then centrifuged at 5000rpm. The supernatant formed was discarded leaving a pure white precipitate of ZnO NPs which was dried in an LD-201-E Vision Scientific Drying oven at 70ºC for 2hrs in order to obtain the desired ZnO Nanoparticles. The procedures are summarized below using a process flow diagram as depicted in Figure 1.

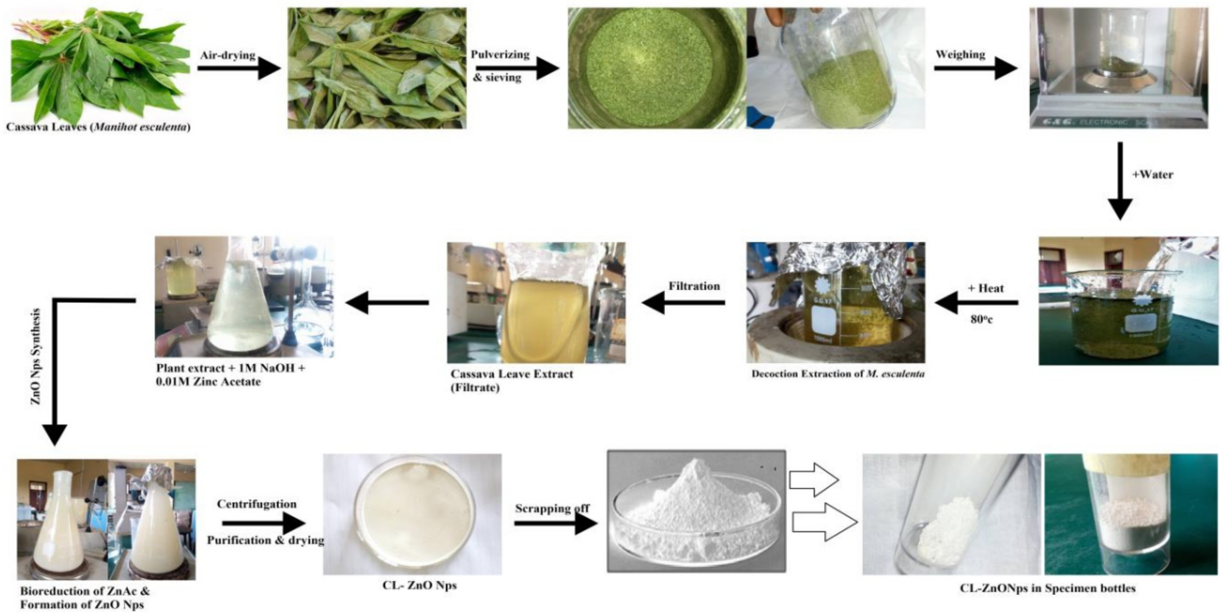

Figure 1: Process flow diagram for the synthesis of Zno nanoparticle from cassava leaf

2.2.7 Corrosion Weight Loss Method

Weight loss measurements were applied to evaluate the efficiency of the synthesized Nano particle (inhibitor), both in the presence and absence of different concentrations of ZnO-NPs. The mild steel metal were immersed for a total of 120hours, with each setup containing 100ppm, 200ppm, 300ppm and a blank (control) removed and weighed after every 24hours to ascertain the subsequent weight loss of the metal. The experimental setup was designed to test the corrosion inhibitory potentials of ZnO NPs from day1 to day5, at 303K.

Results and Discussion

3.1 UV-Vis Spectroscopy

The optical absorption of the ZnONPs as shown in Figure 2 was monitored using UV-Vis spectroscopy. The band was observed between 320 – 500nm of wavelengths, identified as the surface plasmon resonance band. The shape of the band indicated a uniform scattering of the zinc oxide nanoparticles due to the excitation of valence electrons within the nanomaterial. The absorption peak was observed at 371nm [1, 11] reported similar results in their findings.

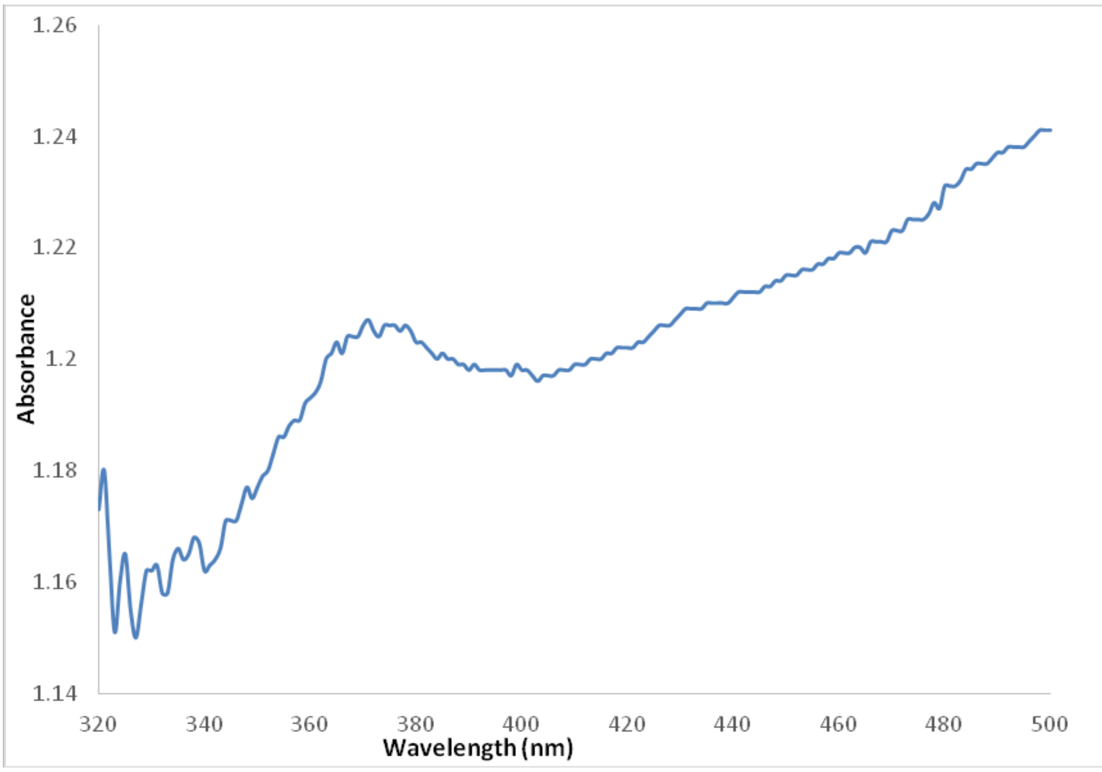

Figure 2: UV-Vis Spectroscopy of CLZnO Nps

3.2 Tauc's Plot (Energy band gap)

The band energy of the synthesized zinc oxide nanoparticle (ZnO NPs) was obtained at E_g=3.3 eV as shown in Figure 3. This provides information about electronic transitions occurring in the material. For semiconductors,the band gap in the absorption spectrum corresponds to the point at which absorption begins to increase from the baseline, since this indicates the minimum amount of energy required for a photon to excite an electron across the band gap and thus be absorbed in the semiconductor material [12]. Fitting a tangent would depend on the shape of the absorption spectrum and according to [12], the procedure is often subjective and may result in error with significant value. Since spectra are typically reported in units corresponding to the wavelength of light rather than its energy, the conversion between wavelength (nm) and band gap energy (eV) units was achieved by the equations 3 – 5 below: [13]

$$\alpha h v\ \alpha\ (\ hv - E_g)^n \quad (3)$$

For direct transition where $n = \frac{1}{2}$

Thus;

$$(\alpha h v)^2 = (2.303 \times Abs \times E_g) \quad (4)$$

Where; Abs = Absorbance and E_g= Band Energy, is given as equation 3;

$$E_g = \frac{hc}{\lambda} = \frac{1239.8}{\lambda}(eV \times nm) \quad (5)$$

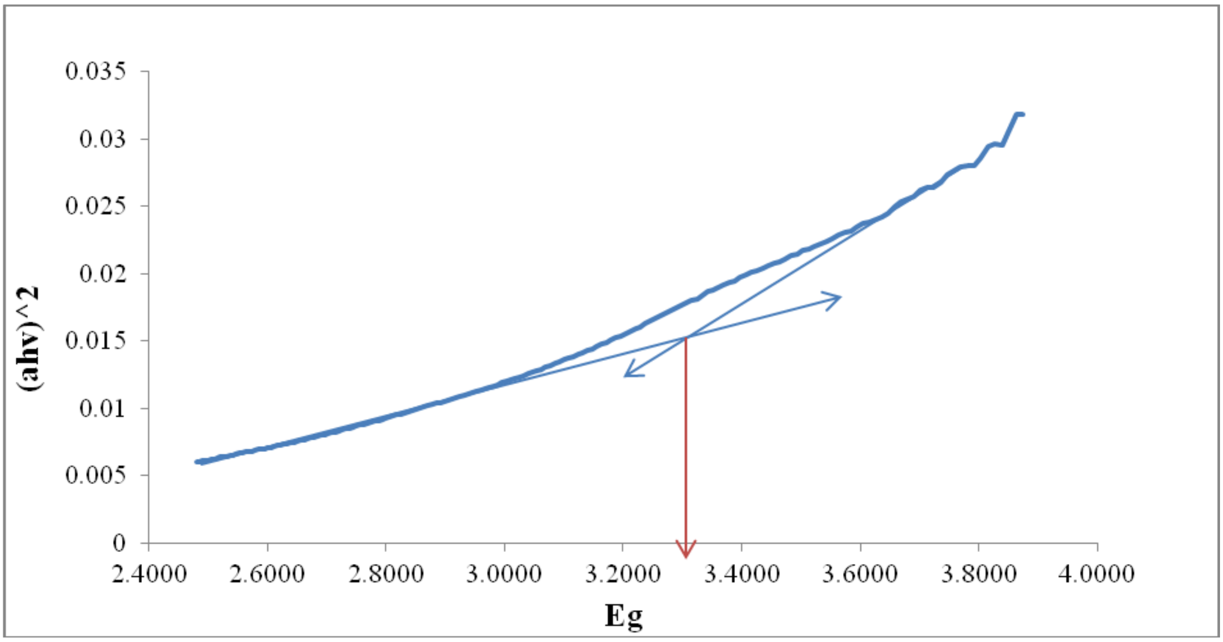

Figure 3: Tauc's plot for CI-ZnO Nps

3.3 Fourier Transform Infra-red Analysis (FTIR)

Figure 4 depict the FTIR result of the ZnONPs. This FTIR gives information on the vibration and rotational modes of motion of a molecule in line with the functional group present in the material and hence an important technique for identification and characterization of a substance. Absorptionpeak 1408.9 cm^{-1} which falls within the range of 1100 - 1600 cm^{-1}indicates Zn – OH bending mode thus corroborating the work of [14]. The peaks of absorption revealed at this wavelength 3380.8cm^{-1}, and 1982.98cm^{-1} showed the presence of –OH, and C=O functional group respectively. The broad band at 2109.7 cm^{-1} indicates bioactive thiamine N=C=S, while the region in the band 1640 cm^{-1} is due to the presence of C=N and C=O bonds.These functional groups indicated are relevant to corrosion inhibitor in the corrosion chemistry. In the work of [15], 756 and 431 cm^{-1} broad bands were used to indicate the presence of Zinc oxide nanoparticle but the band region 890.8 cm^{-1} observed suggest as well the presence of Zinc oxide nanoparticle formation since this value is closer to 887 cm^{-1} reported by [16], as ZnO absorption stretching mode.

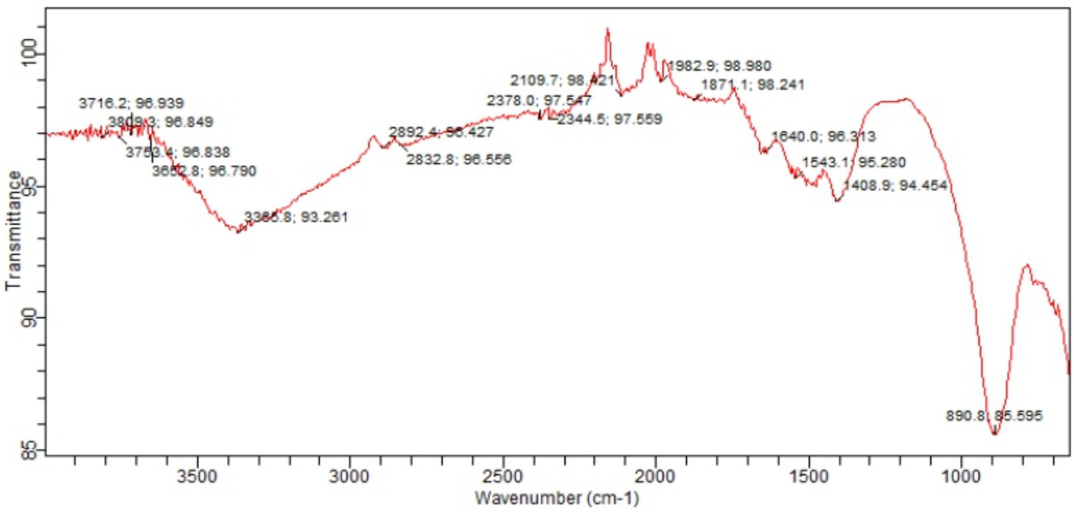

Figure 4: Fourier Infra-red (FTIR) of the CL-ZnO Nps

3.4 Corrosion Potential of ZnONPs (Weight loss)

Figures 5a and 5b showed the weight loss of mild steel in 1.0M HCl in the presence and absence of varying inhibitor concentrations with time of immersion. Figure 5a indicated that the weight loss of mild steel increases progressively as time increases with respect to the inhibitor concentration. From Figure 5b, it is seen that the weight loss decreases as inhibitor concentration increases with exposure time. This may be due to the fact that with increased inhibitor concentration, larger number of molecules of the zinc oxide nanoparticle is adsorbed onto the surface of the mild steel coupon, and the increased adsorption is facilitated by the particle size of the inhibitor, resulting in an increased surface area coverage on mild steel in corrosive medium thereby making it very difficult for the electrolytic solution to further attack the metallic surface. The rate of corrosion decreases with increased in inhibitor concentrations but increases with time as observed. The mild steel corrosion process in acidic medium can be attributed to the presence of OH^-, O_2^+, H^+, and Cl^-. The weight loss in absence of the inhibitor was much significant compared to the weight loss in the presence of the inhibitor. The result thus confirms an inverse proportionality between concentration of ZnONPs and weight loss.

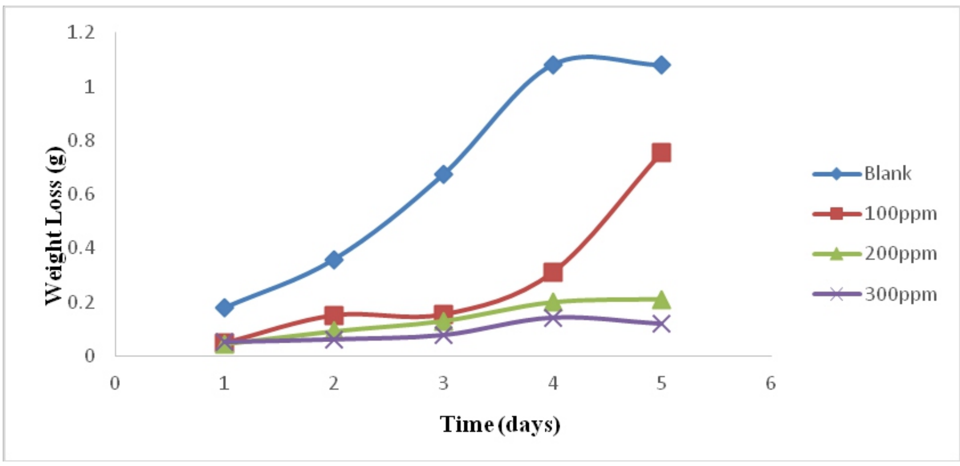

Figure 5a: Weight loss with time for Inhibitor Concentration

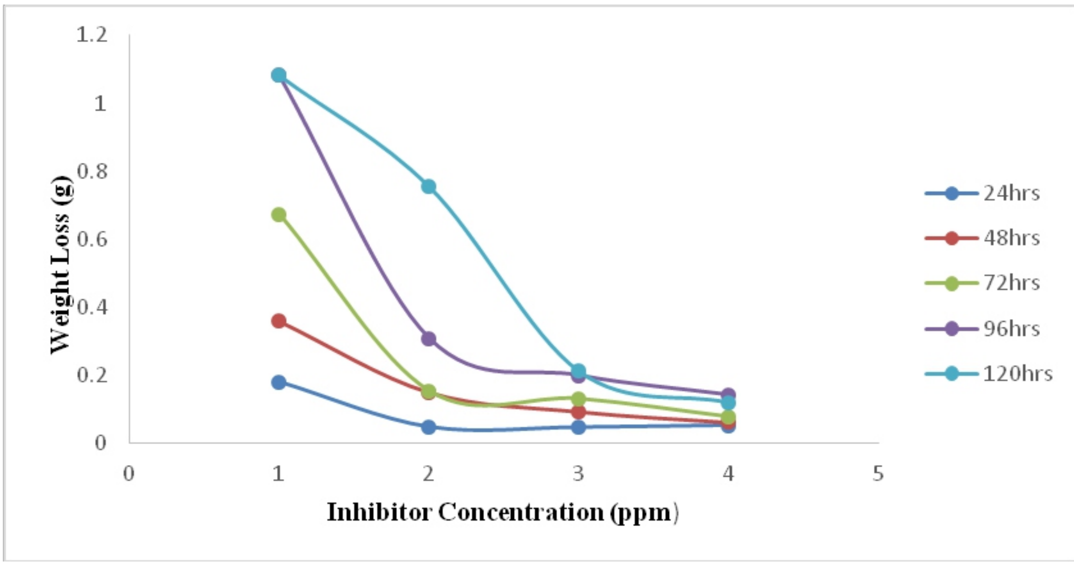

Figure 5b: Weight loss with Inhibitor Concentration at different exposure time.

Corrosion rate (CR) Analysis

The rate of corrosion was determined using equation 6 below;

$$\text{corrosion rate(mpy)} = \frac{kW}{ATD} (6)$$

Where, k is a constant with value as 87.6mpy, W is the weight loss (mg), A is the cross sectional area, T is the time (hr), D is the density of mild steel (g/cm^3). The corrosion rate of mild steel in 1.0M HClin the presence and absence of varying inhibitor concentrations is shown in Figure 6a, this indicates that the corrosion rate decreases with increase in inhibitor concentration from a maximum value of 0.0014 mmpy to 0.00018 mmpy on day 5. This phenomenon is largely attributed to certain physical properties of the Zinc oxide nanoparticles such as; particle size and surface density. These properties facilitated a quantum effect otherwise not experienced in bulk ZnONPs with increased in inhibitor concentration, the zinc oxide nanoparticles get adsorbed onto active sites on the surface of the mild steel coupon, and by virtue of its particle size within the nanoscale region, increased adsorption is continuously facilitated, making it difficult for the acidic medium to further attack the metallic surface. From Figure 6b, it shows the variation of corrosion rate with time for different inhibitor concentrations. Without any inhibitor concentration (blank), it was observed that the corrosion rate occurred distinctively at higher values compared to the inhibitor containing electrolytes. At 72hours on Blank, the corrosion rate reached its maximum and further exposure to the electrolyte resulted in decreasing values. Thus, it can observed that the ZnO NPs tries to literally decrease the distance between the points of initial and maximum corrosion rates, such that the metallic surface experience minimal effects of corrosion rate. Figure 6 also indicated that with increasing inhibitor concentration, the corrosion rate decreases.

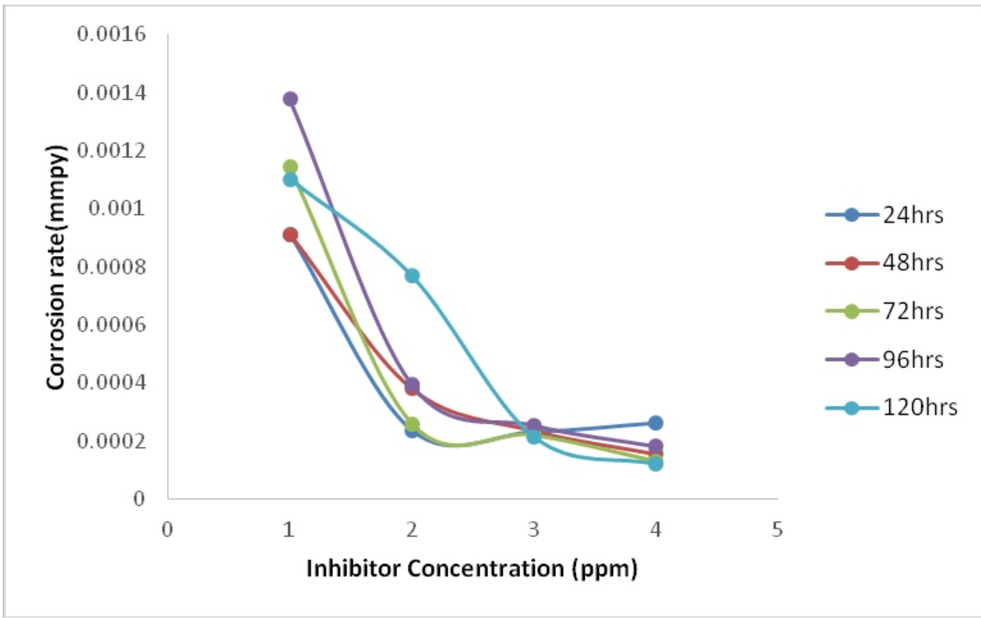

Figure 6a: Variation of Corrosion rate with Inhibitor Concentration at different exposure time.

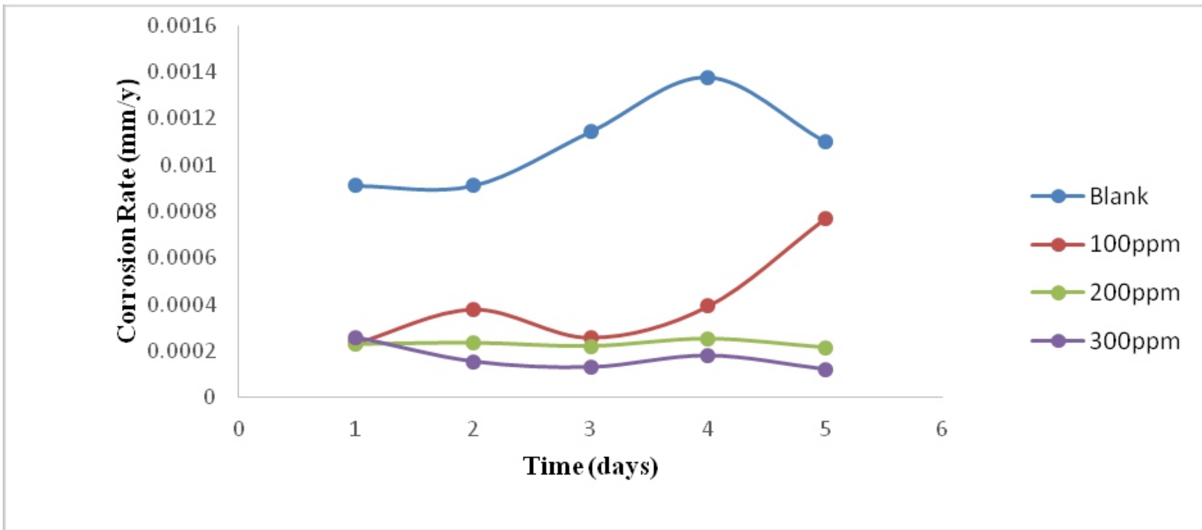

Figure 6b: Variation of Corrosion rate with time for different concentrations of ZnO NPs.

Surface Coverage and Inhibition Efficiency Analysis

Both surface coverage and inhibition efficiency was calculated using equations 7 and 8 respective;y;

$$\text{Surface coverage}(\theta) = \frac{W_A - W_P}{W_A} \quad (7)$$

Where; W_A is Weight loss in the absence of inhibitor (g),W_P is Weight loss in the presence of inhibitor (g)

$$\text{Inhibition Efficiency } (\%) = \frac{W_A - W_P}{W_A} \times 100 \quad (8)$$

Where, W_1 is the weight loss in the absence of inhibitor(g), W_2 is the weight loss in the presence of inhibitor (g).

The surface coverage and inhibition efficiency of zinc oxide nanoparticles on mild steel in 1.0M HCl in the presence and absence of varying inhibitor concentrations is seen in Figures 7a and 7b.This indicated that the surface coverage and inhibition efficiency decreases with increase in inhibitor concentrations while both surface coverage and inhibition efficiency decreased with increase in inhibitor concentration but as time progresses their values increased as well. 100ppm of the zinc oxide nanoparticles represented the least concentration, but at 120 hours of exposure time, it experienced the highest values of surface coverage and inhibition efficiency.

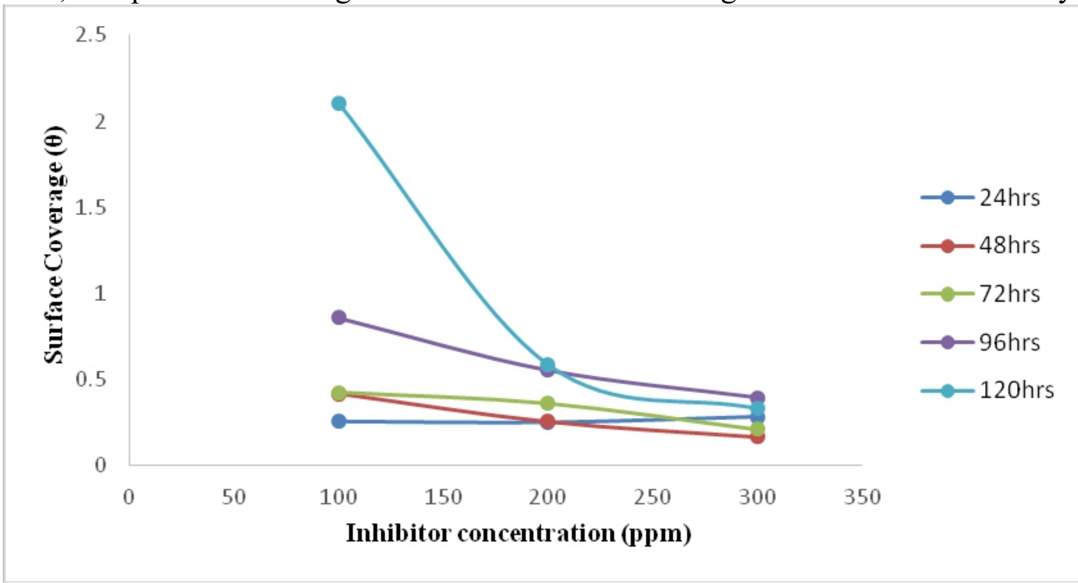

Figure 7a: Variation of Surface coverage with inhibitor concentration at different time interval

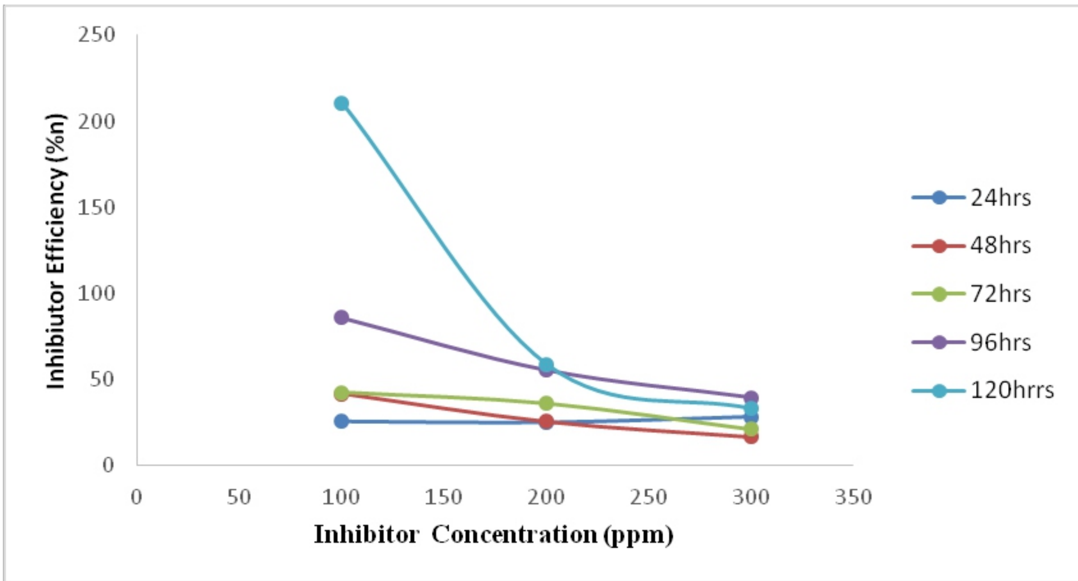

Figure 7b: Variation of Inhibitor Efficiency (%) with Inhibitor Concentration (ppm)

Conclusion

Cassava leaf Zinc oxide Nanoparticle (CL-ZnONPs) was synthesized and used as a corrosion inhibitor on mild steel in acidic medium in this study. Gravimetric method was employed in the weight loss analysis. The effects of contact time, and cassava leaf Nanoparticle concentrations on the corrosion rate, inhibition efficiency, surface coverage, and weight loss of mild steel were determined. Presence of Nitrogen, Oxygen, Carbon, and Sulphur atoms in the functional group of tannins, phenols, flavonoids, and saponins as secondary metabolites of the cassava leaf extract, facilitated the bio-reduction of Zinc acetate into ZnO NPs which makes it to be a good inhibitor on mild steel. The FTIR analysis also proved the presence of these heteroatoms that is responsible for the formation of protective layer on the metal surface. The inhibition efficiency was observed to increase with exposure time and decrease as inhibitor concentrations is increase. The band energy of the synthesized zinc oxide nanoparticle (ZnO NPs) was obtained at E_g=3.3 eV. Corrosion rate of the mild steel decrease with increase in inhibitor concentration from a maximum value of 0.0014 mmpy to 0.00018 mmpy.

REFERENCES

[1]. Vishwakarma, K., (2018), Green Synthesis of ZnO Nanoparticles using Abrus Precatorius Seed Extract and their Characterization, Thesis submitted to the Department of life science, Rouekela, India.

[2]. Subramanian, R., Abdullah, M., and Sadikun, A., (2012), A bitter plant with sweet future? A comprehensive review of an oriental medicinal plant: Andrographis paniculata, Phytochemistry Reviews, 11(1), DoI:10.1007/s11101-011-9219-z

[3]. Dabbs, D.M. and I.A. Aksay, (2000), Self-assembled ceramics produced by complex–fluid templation, Annual Rev. Physical Chem. 51, 601–622.

[4]. Nasrollahzadeh, M., Sajadi, S. M., Sajjadi, M., and Issaabadi, Z., (2019), An Introduction to Nanotechnology, In Interface Science and Technology, 1st Ed., Vol., 28, Elsevier Ltd, ISBN: 9780128135860, https://doi.org/10.1016/B978-0-12-813586-0.00001-8

[5].Herlekar, M., Barve, S., and Kumar, R., (2014), Plant-Mediated Green Synthesis of Iron Nanoparticles, Journal of Nanoparticles, Volume 2014, https://doi.org/10.1155/2014/140614.

[6].Chaudhuri, S. K., and Malodia, L. (2017), Biosynthesis of zinc oxide nanoparticles using leaf extract of *Calotropis gigantea*: characterization and its evaluation on tree seedling growth in nursery stage, Applied Nanoscience, 7, 501 – 512.

[7]. Balamurugan, V., Sheerin, F. M. A., and Sreenithi, V., (2019), A guide to phytochemical analysis, International Journal of Advance Research and Innovative Ideas in Education, 5, 236-245.

[8]. Odeja, O., Obi, G., Ene Ogwuche, C., Elemike, E. E., and Oderinlo, Y., (2015), Phytochemical screening antioxidant and antimicrobial activities of senna occidentalis (L) leaves extract, Journal of clinical phytoscience, 2 – 6.

[9]. Haque, M. J., Bellah, M. M., Hassan, M. R., and Rahman, S., (2020), Synthesis of ZnO nanoparticles by two different methods and comparison of their structural, antibacterial, photocatalytic and optical properties, Iop, Nano express, 1, 010007, https://doi.org/10.1088/2632 959x/ab7a43.

[10].Elemike, E. E., Damian, O., Anthony, C. E., Sonde, C. U., and Ehiri, R. C., (2017), Green Synthesis of Ag/Ag2O Nanoparticles Using Aqueous Leaf Extract of Eupatorium odoratum and Its Antimicrobial and Mosquito Larvicidal Activities, Molecules, 22(5): 674, DOI:**10.3390/molecules22050674**.

[11].Shabnam, F., Jamzad, M., and Hassan, K. F., (2019), Green synthesis of zinc oxide nanoparticles: a comparison, Green chemistry letters and reviews, 12(1): 19 – 24.

[12].Chen, Z., and Jaramillo, T. F., (2017), The Use of UV-visible Spectroscopy to Measure the Band gap of a Semiconductor, Edited by Bruce Brunschwig, Department of Chemical Engineering, Stanford University.

[13]. Tauc, J., (1972), Optical Properties of Solids," Abeles, North Holland, Amsterdam.

[14].Das, J., Evans, I. R., and Khushalani, D., (2009), "Zinc Glycolate: A Precursor to ZnO," Inorganic Chemistry, Vol. 48, No. 8, 2009, 3508-3510. doi:10.1021/ic900067

[15]. Al-Senani, G. M., (2020), Synthesis of ZnO-NPs using a Convolvulus arvensis leaf extract and
proving its efficiency as an inhibitor of carbon steel corrosion, Materials, 13(4), 890 https://doi.org/10.3390/ma13040890.

[16]. Nakamoto, K., (1997), Infrared spectra of inorganic and coordination compounds, Wiley, New York.